Molecular simulation of perfluorohexane adsorption in BAM-109 activated carbon

Adsorption Science & Technology

Article

Molecular simulation of perfluorohexane adsorption in BAM-109 activated carbon

Adsorption Science & Technology
0(0) 1–22

DOI: 10.1177/0263617415619526
adt.sagepub.com
SAGE

Lev Sarkisov
The University of Edinburgh, UK

Abstract
In this study we construct micro- and micro-mesoporous models of activated carbon BAM-109. The model is based on random packing of structural elements, here provided by hydroxyl-functionalized corannulene molecules. The properties of the model are tuned to reflect structural characteristics of the reference material and its adsorption behaviour. Using the proposed model (the mesoporous variant of it) we predict that BAM-109 should adsorb 40.84, 45.05, 50.12 cm^3 (STP)/g of perfluorohexane at 0.1, 0.3 and 0.6 relative pressures, respectively, at 273 K. These results are then compared to the reference experimental data. Although simulations correctly predict the trend in the adsorption density, the model, in its current form, systematically underestimates adsorbed density by 20% on average. We reflect on the deficiencies of the model and possible strategies to improve it.

Keywords
adsorption, simulation, activated carbon, industrial challenge

Introduction

Despite several decades of research, construction of accurate predictive models of adsorption in activated carbons remains one of the most difficult and largely unanswered challenges. Yet, these models could be of a tremendous help in the development and optimization of adsorption processes. Given recent interest in these processes as an energy efficient platform for carbon capture (Ebner and Ritter, 2009; Samanta et al., 2012; Wang et al., 2011), energy storage and other applications, it becomes important to assess the current state of the art in molecular models of activated carbons and other disordered materials and to identify the key bottlenecks in the development of predictive approaches.

Hence, this is the topic of the Eighth International Fluid Properties Simulation Challenge. The objective of the challenge is to predict adsorption of perfluorohexane in BAM-109

Corresponding author:
Lev Sarkisov, Institute for Materials and Processes, School of Engineering, The University of Edinburgh, EH9 3JL Boise, Edinburgh, UK.
Email: Lev.Sarkisov@ed.ac.uk

activated carbon at 273 K. BAM-109 is known for its highly reproducible adsorption properties and consistency of samples. This property of BAM-109 enabled it to be certified as a reference material. A number of properties of BAM-109 have been measured and provided as the reference data by the challenge organizers, including argon adsorption and desorption isotherms at 87 K; carbon dioxide adsorption isotherm at 273 K; water adsorption and desorption isotherms at 293 K; pore volume, pore size distribution (PSD) and surface area obtained from the non-local DFT (NLDFT) (Ravikovitch et al., 2000), quenched solid DFT (QSDFT) (Neimark et al., 2009) and Brunauer–Emmett–Teller (BET) (Brunauer et al., 1938) methods, X-ray diffraction, X-ray photoelectron spectroscopy and elemental analysis.

The idea is to use this information to construct and calibrate the molecular model of BAM-109. For this, there are several avenues at our disposal. The model which has most commonly been used to describe activated carbons is the slit pore model (Bandosz et al., 2003; Everett and Powl, 1976). Based on the experimental evidence of the lamellar pore structure in many carbons, it treats porous space as a collection of independent slit pores, with the pore walls made of an infinite number of graphite sheets. Adsorption in individual slit pores is linked to the adsorption in whole sample through the adsorption integral equation (AIE). If adsorption isotherms in individual slit pores of particular widths are known (forming so-called adsorption kernel), the AIE equation can be inverted to obtain a PSD and this PSD can then be used for prediction of adsorption in this material at other conditions or for other species and mixtures of species (for a brief review of the method, see Vega, 2007).

This approach has been applied to investigate adsorption of different light gases in activated carbons, including CO_2, N_2, CH_4 and H_2O, as well as binary and ternary mixtures (Cracknell et al., 1996; Heuchel et al., 1999; Jagiello and Schwarz, 1993; Kaneko et al., 1994; Lithoxoos et al., 2012; McCallum et al., 1998; Samios et al., 1997; Silvestre-Albero et al., 2012; Sweatman and Quirke, 2001). Many variants of the slit pore model have been developed over the years to incorporate various sources of heterogeneity in the structure, including walls of finite size and pores of finite length, surface groups, defects and so on (Brennan et al., 2002; Coasne et al., 2006; Do and Do, 2006; Gotzias et al., 2012; Jagiello and Olivier, 2009; Jorge et al., 2002; Jorge and Seaton, 2003; Kandagal et al., 2012; Liu and Wilcox, 2012; Lucena et al., 2010; McCallum et al., 1998; Müller et al., 1996; Vishnyakov et al., 1998; Wongkoblap and Do, 2006, 2007). The principal challenge in application of this approach is the reliability and realism of the PSD. Inversion of the AIE is an ill-posed problem and either no or an infinite number of PSDs can in principle satisfy the equation and various procedures have been devised to guide the search for the most reliable PSDs. Nevertheless, the PSDs obtained by using different species generally differ from each other and predictions typically remain accurate only for similar species and in a narrow window of temperature and pressure conditions.

An improved strategy has been proposed in a series of recent studies by Sweatman and Quirke showing that very accurate predictions can be obtained for light gases adsorbing in a number of activated carbons (Sweatman and Quirke, 2001, 2005; Sweatman et al., 2006). For this, two aspects of their protocol are particularly important. First, they chose a reference microporous carbon and used carbon dioxide at 293 K adsorption data to obtain a robust PSD (in other words, the resulting PSD is the least sensitive distribution to perturbations in the experimental data or the kernel out of all possible PSDs that fit the experimental data within the experimental error). Second, they

used this PSD and experimental data for adsorption of other species on the reference microporous carbon to tune the parameters of the solid–fluid interactions for this species until a good match with the experimental data is obtained. The basic idea is that the details of solid–fluid interactions should be similar for all microporous activated carbons and the obtained parameters are thus transferrable. To predict adsorption in other materials at various temperature and pressure conditions only a PSD from carbon dioxide at 293 K is required for that specific material. This approach is clearly not applicable here as perfluorohexane is a substantially more complex species than the species for which the reference data have been provided and there are no optimized solid–fluid interaction parameters available for this system.

Interestingly, adsorption of linear alkanes and other hydrocarbon species in carbonaceous slit pores is a substantially less explored subject, compared to light gases in activated carbons or hydrocarbons in zeolites, with only few articles published recently (Harrison et al., 2014; Pinto da Costa et al., 2011; Severson and Snurr, 2007). Thus the accuracy of the approaches based on the slit pore model in application to adsorption of hydrocarbons and other more complex species is yet to be established.

On the other side of the spectrum of available approaches, are models which attempt to capture the disordered structure of activated carbons in its full complexity by either imitating the process of material formation or by reproducing simultaneously several key structural characteristics, such as radial distribution functions, surface area and density (Brennan et al., 2001; Kumar et al., 2011; Nguyen et al., 2008; Palmer et al., 2009; Thomson and Gubbins, 2000; Walters et al., 1995). These models tend to be computationally demanding. Other challenges include systematic assignment of partial charges in the atoms of the structure, incorporation of the surface groups and limited number of structure realizations due to computational constraints.

Both of the approaches have a number of champions in the community. To complement this picture here we adopt yet another route to model disordered activated carbon structures, based on a random distribution of structural fragments. In a more general form, where the solid structure is represented as a random distribution of particles, this approach has played a prominent role in fundamental studies of confined fluid phase behaviour (Gelb et al., 1999). It has been argued that the structure of many disordered activated carbons is composed of smaller structural units, such as several fragments of graphene stacked together (so-called basic structural unit (Oberlin et al., 1980)). This notion can be combined with well-established theoretical and simulation approaches, where disordered porous materials are represented as a collection of randomly distributed structural elements. One of the earlier examples of this approach is the model proposed by Segarra and Glandt (1994). The basic element of this model is a platelet, or a rigid disk, representing a stack of several (between one and three) fragments of a carbon layer. Adsorbate–adsorbent interactions are described by developing a potential function for a platelet of a limited size in a fashion similar to the procedure required for the Steele 10-4-3 potential (Steele, 1978). The complete model considers a random packing of these platelets. This model was employed in grand canonical Monte Carlo simulations of methane and ethane adsorption, and as well as adsorption of water vapour. Liu and Monson further developed the model by Segarra and Glandt to accurately reflect specific structural characteristics of BPL carbon (Liu and Monson, 2005). In their model the size of the platelet (1.7 nm) and the porosity of the structure corresponded to the existing experimental values. The original work was based on the structureless platelets and effective potentials, similar to that of Segarra and Glandt,

while in the second phase of the work carbonylic groups and Coulombic interactions associated with them were modelled explicitly (Liu and Monson, 2006).

In a similar spirit, many other realistic models have been developed over the years. The presence of curved, fullerene-related elements due to non-hexagonal rings is now widely accepted and has been subject of extensive studies (Hawelek et al., 2008; Klauda et al., 2004; Radovic, 2004; Radovic and Bockrath, 2005). These elements have been directly observed in high resolution electron microscopy experiments and introduced in theoretical models (Harris, 2004, 2005; Harris et al., 2000; Harris and Tsang, 1997). In particular, Terzyk and co-authors have compared different methods for the determination of the PSD in a structure made of fragments of this type, while Kowalczyc and co-authors have studied the displacement of methane by carbon dioxide on different types of Schwartzites (Kowalczyk et al., 2012; Terzyk et al., 2007). Kumar and co-authors have investigated the mixtures CH_4/H_2 and CH_4/N_2 in different models for microporous carbon, including a random arrangement of coronene graphitic basic units (Kumar et al., 2012).

Recently, we adopted this approach to construct models of high surface area activated carbons, with a view to explore the properties of these models in the context of carbon capture processes (Di Biase and Sarkisov, 2013). The model, based on a random packing of corannulene molecules functionalized with two hydroxyl groups, was tuned to capture experimentally measured surface area and pore volume of the reference material (Maxsorb MSC-30). Although solid–fluid interactions with molecules featuring no partial charges (methane, hydrogen) required some scaling, the model was able to accurately reproduce adsorption of carbon dioxide, nitrogen, hydrogen and methane within a reasonable window of conditions, relevant for the carbon capture processes. Later, this approach was applied to multi-component mixtures, including water, corresponding to industrial streams and conditions associated with carbon capture (Di Biase and Sarkisov, 2015).

In comparison, with two other approaches described earlier, the approach based on random packing of structural elements seems to strike a reasonable compromise. Although it is not as accurate as the state-of-the-art approaches based on slit pore models, it provides a simple route to generate structures with realistic surface areas and structural heterogeneity. It does not require generation of a kernel of isotherms (which may become computationally demanding for more complex species and this kernel is also required for each new temperature). It allows easy addition of structural heterogeneities such as surface groups. Compared to more realistic models of activated carbon, based on the reverse Monte Carlo methods, the fragment-based approach is computationally more tractable, and partial charges on atoms, including functional groups, can be easily calculated using Quantum-Mechanical (QM) methods on individual fragments. We also note that the idea to construct model carbons with the predetermined characteristics is similar in spirit to the concept of virtual carbons introduced by Biggs and Buts (2006).

Methodology

General strategy

Our overall strategy is as follows. Similarly to our previous studies, we consider a molecule of corannulene as a structural element. The molecule consists of a central cyclopentane ring surrounded by five benzene rings. It has a bowl-like shape and can be considered as a fragment of fullerene, C_{60}. X-Ray photoelectron spectroscopy data indicate between 2.6 and 4.6% atomic concentration of surface oxygen in BAM-109. To incorporate this data

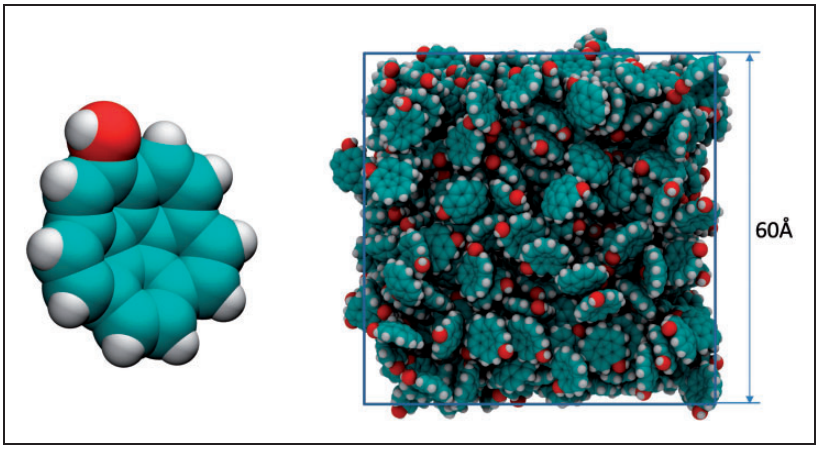

Figure 1. On the left: computer visualization of a single molecule of corannulene, functionalized with a hydroxyl group, used as a basic structural element. On the right: computer visualization of a random packing of 395 structural elements in a simulation box of 60 Å in size. In this picture and throughout the article, cyan is for carbon, red is for oxygen, light grey is for hydrogen.

into the model, we functionalize corannulene molecule with a single hydroxylic group, as shown in Figure 1, giving the total oxygen atomic concentration of 4.7% (excluding hydrogen).

As a model of a porous material we consider a random packing of these structural elements. High surface area of corannulene allows for an easy modulation of the properties of the packings, such as the surface area and pore volume, by removing some of the structural elements from a dense configuration. The idea is to bring the properties of the random packing as close to the experimentally measured values as possible. Surface area and pore volume are not independent properties and their values cannot be tuned separately from each other. The contest objective is to reproduce perfluorohexane adsorption at 0.1 and 0.3 relative pressures at 273 K (and at 0.6 relative pressure using a model that accounts for mesoporosity in the sample). From our experience in the studies of alkane adsorption in activated carbons, at 0.1 and 0.3 relative pressures, adsorption of perfluorohexane should be very close to the micropore volume capacity and therefore, to reproduce these points, the primary target of the model is the micropore volume with the surface area being the secondary characteristic.

Once the structure with the desired properties is obtained, grand canonical Monte Carlo simulations are employed to generate adsorption isotherms for argon, carbon dioxide, water and perfluorohexane. The simulation predictions are compared to the experimental data provided by the organizers of the Eighth Industrial Fluid Properties Simulation Challenge, referred throughout as the reference data.

Force field details

The full set of Lennard-Jones (LJ) parameters associated with the adsorbent is reported in Supplementary Information (SI). The LJ parameters mostly coincide with the ones proposed by Tenney and Lastoskie (2006), which are in line with other parameters reported in

literature. These are the parameters also used in our previous work (Di Biase and Sarkisov, 2013). Structural optimization of hydroxyl-functionalized corannulene and partial charges on the atoms are obtained using the B3LYP Density Functional Theory method (Axel, 1993), 6-31G basis set and CHELPG charge analysis (Breneman and Wiberg, 1990) with the Gaussian 09 software package (Frisch et al., 2009).

We use the TraPPE force field for carbon dioxide and perfluorohexane (Potoff and Siepmann, 2001; Zhang and Siepmann, 2005), TIP4P model of water (Jorgensen and Madura, 1985) and a well-known model for argon (Hirschfelder et al., 1954). Details of the models (such as the geometry of the molecules, LJ parameters, partial charges) and saturated pressures at relevant temperatures are provided in the SI.

LJ parameters for cross-species interactions are calculated using the standard Lorentz–Berthelot rules (arithmetic average for the collision diameters and geometric average for the well depths). It has been proposed that the LJ interactions emanating from the curved carbon surfaces are stronger than that from the flat carbon sheets due to mixed sp^2–sp^3 hybridization states of the carbon atoms within curved surfaces (Klauda et al., 2004). Here all values for the well depths of solid–fluid LJ interaction are scaled with 1.1 factor which is consistent with the previous studies (Palmer et al., 2009). In principle, this scaling can be seen as another optimization parameter (Di Biase and Sarkisov, 2013); however, this is outside the scope of this study. All LJ interactions are truncated at the cut-off distance of 13 Å with no long-tail corrections applied.

Simulation methods and parameters

The basic simulation system is a cubic box with side of 60 Å in length, placed in the periodic boundary conditions. Structural characteristics of the packing, including surface area, pore volume, PSD are obtained with the Poreblazer v3.0.2 simulation suite, using the methods summarized in our previous publication (Sarkisov and Harrison, 2011).

Grand canonical Monte Carlo simulations are performed using MuSiC simulation package (Gupta et al., 2003). LJ interactions between atoms of different types and the solid structure are pre-calculated and stored as potential maps with the resolution of 0.2 Å. The same resolution is also adopted for the pre-calculated electrostatic interactions, based on the Ewald summation method (Ewald, 1921). Electrostatic fluid–fluid interactions are obtained from the Fennel–Gezelter method with 13 Å cut-off (Fennel and Gezelter, 2006).

Water and carbon dioxide are treated as rigid molecules. Energy-bias insertions and deletions, using pre-calculated potential maps (Snurr et al., 1993), and random translations are considered for argon, water and carbon dioxide. In addition, random rotations are applied to carbon dioxide and water molecules. All types of moves have equal weighting. Configurational-bias Monte Carlo is employed for simulation of adsorption of perfluorohexane, using the variant of the technique proposed by Macedonia and Maginn (1999). We employ configurational bias Monte Carlo combined with the energy bias method, as proposed by Snurr et al. (1993) and implemented in the MuSiC simulation package (Gupta et al., 2003).

As has been shown in our previous studies, the system is sufficiently large for the properties to become insensitive to a particular realization of the matrix (Di Biase and Sarkisov, 2013). Therefore, all adsorption results correspond to one configuration of packed elements. Each point on adsorption isotherm required between 2×10^7 and 5×10^8 trial moves, depending on the system, with 25–50% of the trial moves used to obtained the

average loading. We note here that this number of steps is not adequate to simulate adsorption of water; however, given the disappointing preliminary results for water (see below) we did not pursue the full convergence of the simulation data for water. Statistical error in loading is calculated as the square root of variance (standard deviation) of the ensemble average. To estimate the latter property, a standard approach based on block averages is employed (Frenkel and Smit, 2002).

Results

Microporous model

Several variants of the general model presented in the methodology have been explored in the preliminary studies. Here we focus on the results for a specific model with the structural characteristics summarized in Table 1. The experimental values are provided in the reference data for the contest (we keep the original precision of the values in the table).

From this table it is clear that the current model captures the microporous volume of the structure reasonably well, however substantially underestimates the surface area. We will revisit the latter property using a mesoporous variant of the current model in the next section. In our previous work, we also explored the relation between pore volumes obtained from the helium porosimetry and from the Dubinin–Radushkevich method (Dubinin and Radushkevich, 1947) applied to model microporous disordered structures. Here we apply the Dubinin–Radushkevich method using experimental data on argon adsorption at 87 K (see SI). The obtained value of 0.569 cm^3/g is somewhat larger than the values reported in Table 1 from QSDFT and from the computational helium porosimetry on the model structure.

Figure 2 shows the normalized PSD of the model structure as a function of pore diameter. The structure is clearly microporous, with the available pores not exceeding 10 Å in size. Comparing to the reference PSDs, obtained using NLDFT and adsorption data for carbon dioxide and argon, the model seems to capture reasonably well the existence of the pores up to 9 Å but fails to incorporate an additional band of pores, between 10 and 20 Å as revealed by argon at 87 K measurements. Given the nature of the model, this is an expected result and we will return to the issue of larger pores in the next section.

Let us now focus on the adsorption results. Figure 3 compares isotherms for argon at 87 K from molecular simulations and reference experimental data. The model has a reasonable performance at very low pressures, overpredicts adsorption in the 10^{-4}–10^{-1} P/P_0 range and starts underpredicting adsorption at higher pressures. This is not an

Table 1. Structural characteristics of BAM-109 from experiments and from the model. In this table *N* is the number of structural elements in the system, *S* is the surface area, *V* is the micropore volume (the experimental value has been obtained from QSDFT analysis of argon adsorption data at 87 K), ρ is the density of the material, *PLD* is the pore limiting diameter and *LP* is the diameter of the largest pore in the structure.

	N	S (m^2/g)	V (cm^3/g)	ρ (g/cm^3)	PLD (Å)	LP (Å)
Experiments	*	1383	0.5163	*	*	*
Model (Micro)	395	990.62	0.509	0.808	4.36	8.45

*Property not applicable, or provided.

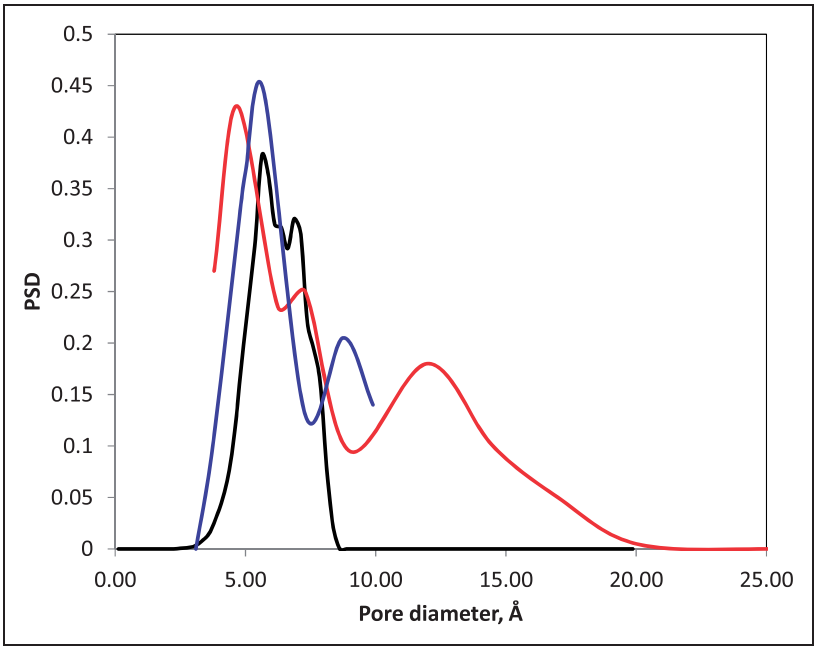

Figure 2. Pore size distribution (arbitrary units) as a function of pore diameter (Å). Black line is computational predictions for the microporous model in this work; red line is from the NLDFT analysis of argon at 87 K isotherm (approximate redrawing of the reference data); blue line is from the NLDFT analysis of carbon dioxide at 273 K isotherm (approximate redrawing of the reference data). Pores in the mesoporous region seen between 10 and 25 nm from the QSDFT analysis of argon at 87 K isotherm (reference data) are not shown.

uncommon pattern for intrinsically microporous models, trying to reproduce experimental behaviour of a material, featuring mesopores. For example, we observed a similar trend for nitrogen adsorption at 77 K in model of Maxsorb MSC-30 (Di Biase and Sarkisov, 2013). Again, a similar pattern was seen for a realistic model of BPL by Palmer et al. (2009).

Carbon dioxide at 273 K results are presented in Figure 4. The model exhibits a reasonable performance at lower pressures but overpredicts adsorption at higher pressures, with the error reaching about 12% at the highest pressure value.

The model is not as accurate with respect to carbon dioxide adsorption as well-calibrated slit pore models. However, it shows a reasonable accuracy (in the microporous region) across very different species and conditions (argon at 87 K, CO_2 at 273 K), it has no adjustable parameters (given that 1.1 solid–fluid scaling factor has been taken from the literature and not optimized) and it does not require generation of a kernel of adsorption isotherms. Further improvement of the model is possible through a more systematic variation of the structural characteristics (surface area, porosity), solid–fluid interactions and choice of structural elements; however, this is not pursued here. In the next section, we will demonstrate that *some* improvement is possible simply by inclusion of mesoporous regions of the structure.

The situation is less encouraging in the case of water (Figure 5). At lower pressures adsorption of water is somewhat overestimated, however, at higher pressures the model

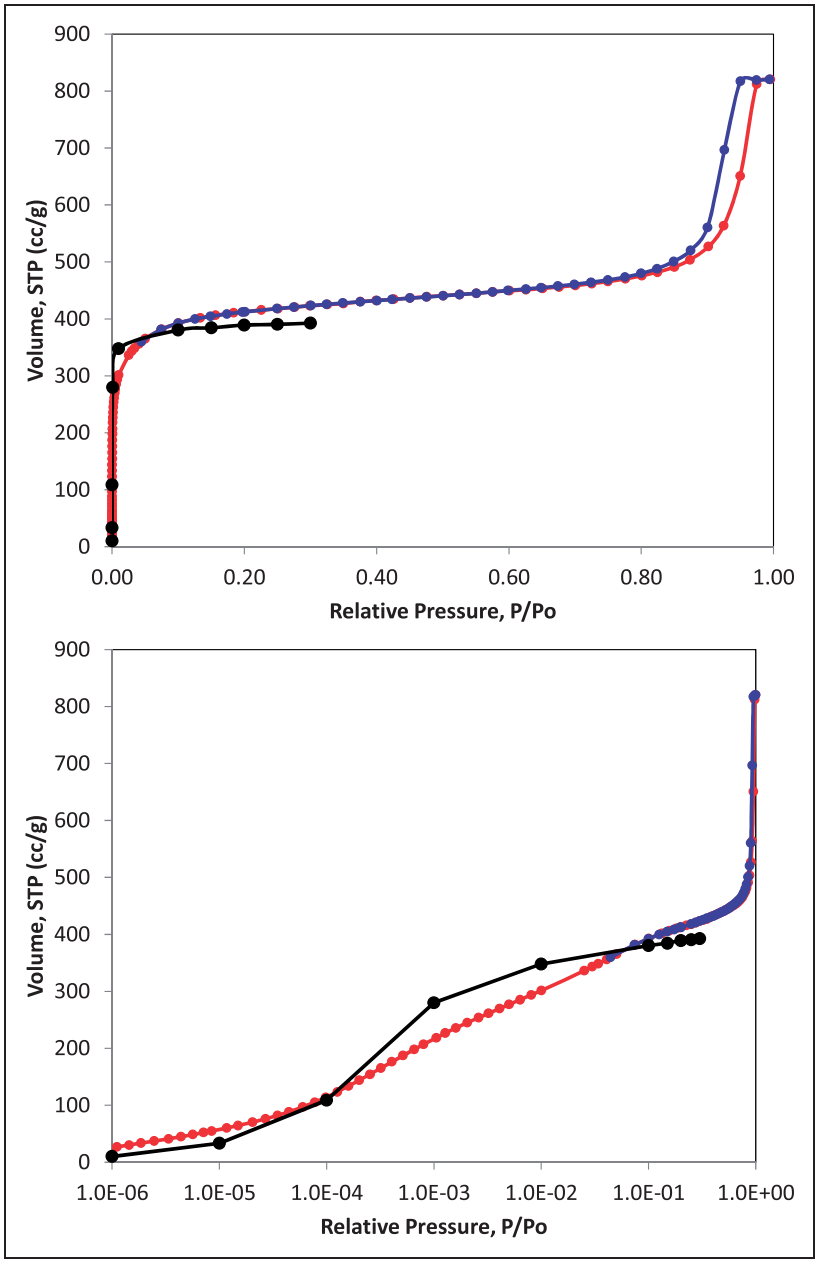

Figure 3. Sorption isotherms for argon at 87 K. Red and blue symbols and lines are the experimental adsorption and desorption isotherms, respectively. Black symbols and line are molecular simulation results. The bottom figure plots the same comparison, using the logarithmic scale for relative pressure.

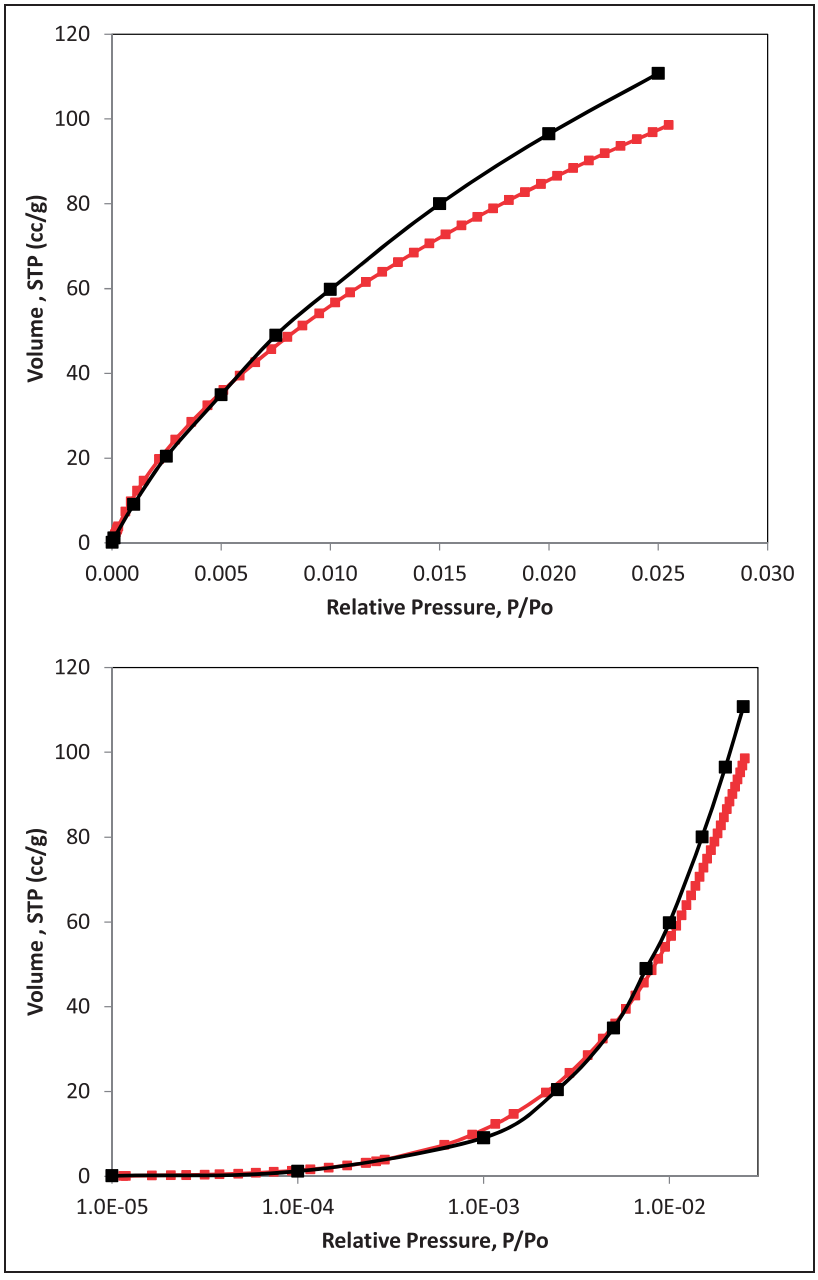

Figure 4. Adsorption isotherms for carbon dioxide at 273 K. Red symbols and line are the experimental results. Black symbols and line are molecular simulation results. The bottom figure plots the same comparison, using the logarithmic scale for relative pressure.

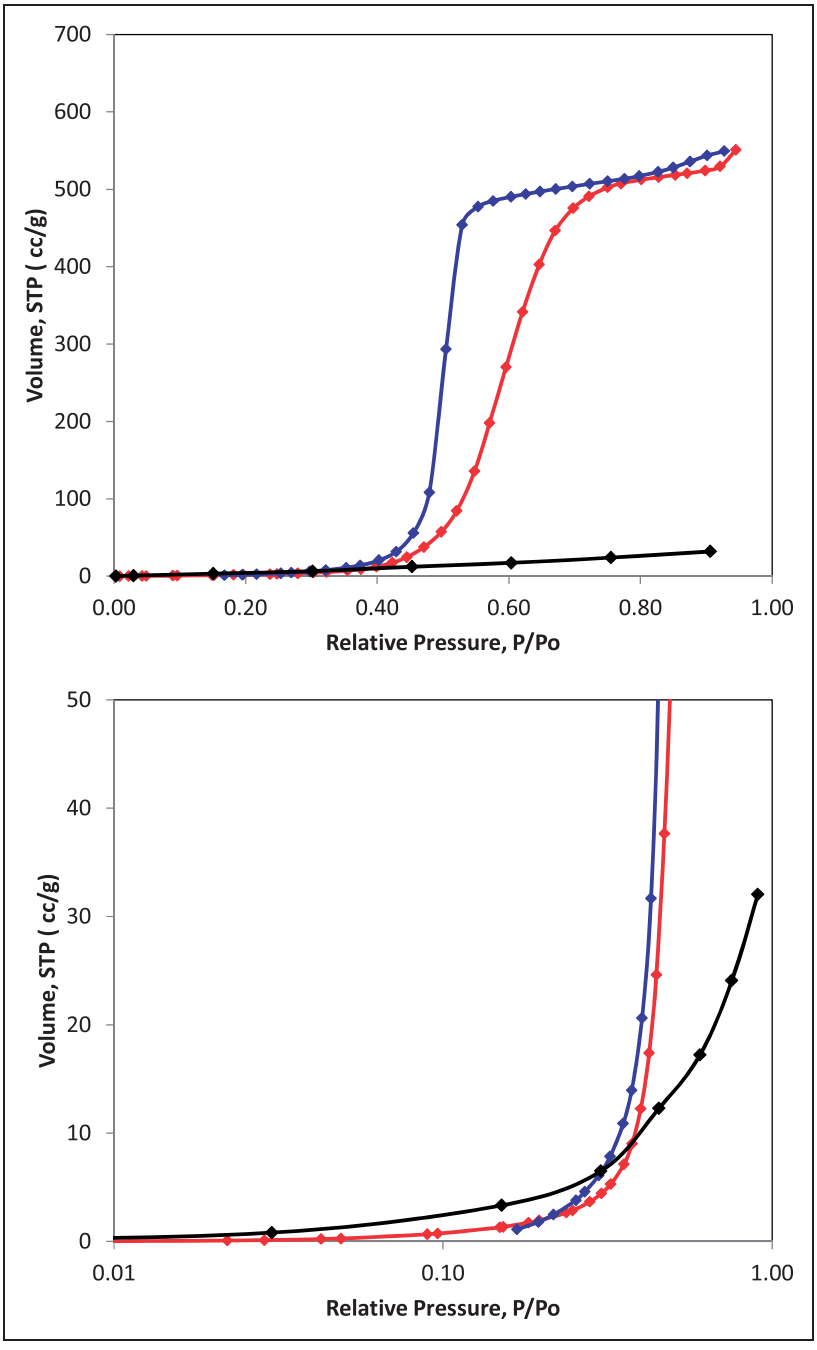

Figure 5. Adsorption isotherms for water at 293.15 K. Red symbols and line are the experimental results. Black symbols and line are molecular simulation results. The bottom figure plots the same comparison, using the logarithmic scale for relative pressure.

fails to capture condensation of water in the pores. In the light of previous attempts to model adsorption of water in activated carbons, this result is hardly surprising. Adsorption of water is initiated on the surface groups of the structure followed by growth and coalescence of the clusters. The process is very sensitive to the surface concentration of the groups, their type and other factors. In our previous study, we simulated adsorption of water (TIP4P) in a model of Maxsorb MSC-30 and observed that the adsorption isotherm is also shifted to larger pressures, compared to the reference experimental results and that general behaviour of water is sensitive to how the surface groups are modelled (Di Biase and Sarkisov, 2015). Specifically, absence of any surface groups makes the model material extremely hydrophobic with the condensation taking place at pressure values beyond the bulk vapour pressure. Given the well-recognized complexity of the water sorption in disordered carbonaceous materials, further investigation of this problem is beyond the scope of the analysis here.

With the comparison between the model predictions and the reference data completed, we now provide the figures for the perfluorohexane adsorption at 273 K (Table 2).

From this table it is evident that the majority of micropores of the model structure are occupied at pressures much lower that the first point required for the contest (0.1). Furthermore, very little additional adsorption occurs at relative pressures beyond 0.1. A typical configuration in this regime is shown in Figure 6. We acknowledge that the current model should have lower volume of micropores accessible to perfluorohexane, compared to the real material. Indeed, the model PSD does not feature any pores in 9–20 Å range that could play an important role in accommodation of perfluorohexane. Thus, the model is likely to underestimate adsorption at 0.3 and 0.6 relative pressures and overestimate adsorption at lower pressures. This issue will be revised in the context of a mesoporous variant of the model. We conclude this section with a representative snapshot of the system fully saturated with perfluorohexane.

Micro-mesoporous model

Although several strategies could be contemplated to incorporate mesopores into the model, here we adopt a simple (but most likely not very accurate) approach. Specifically we consider random packings of structural elements intercalated with empty regions representing mesopores. The idea is to adjust the size of the empty regions so that the total pore

Table 2. Volume of perfluorohexane (cm^3/g STP) adsorbed in a model BAM-109 structure at 273 K as a function of relative pressure. P_0(T = 273 K, TraPPE) = 34.8 kPa, see SI. Statistical error in loading at target pressures does not exceed 3%.

P/P_0	V (cm^3/g STP)
0.003	36.57
0.014	38.32
0.029	39.00
0.057	39.82
0.100	42.38
0.300	43.37
0.600	43.43

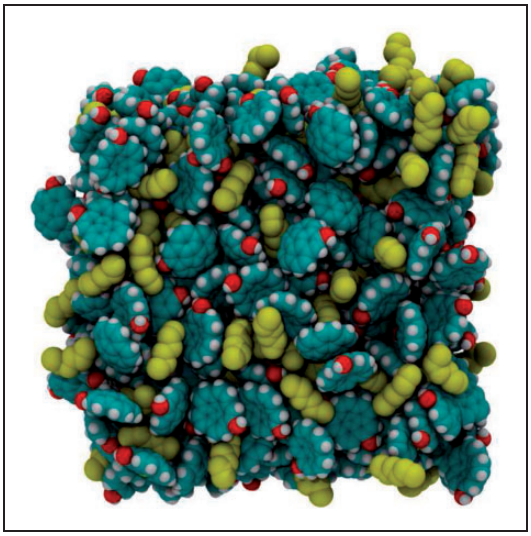

Figure 6. Computer visualization of the state of the system saturated with perfluorohexane (shown in yellow, 203 molecules). Other colours as before.

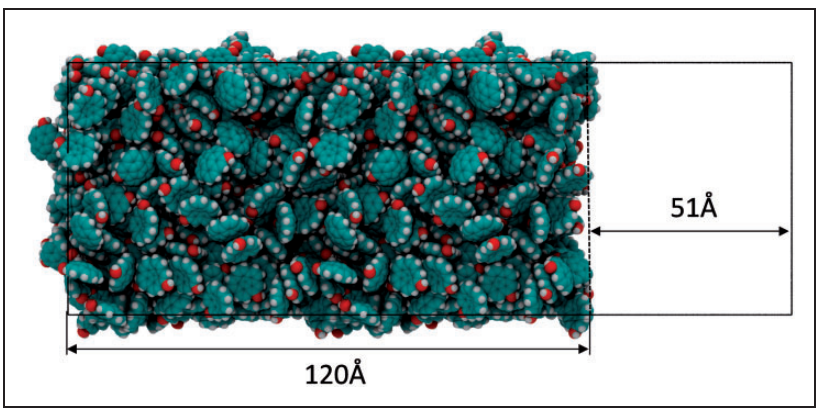

Figure 7. Computer visualization of a random packing of structural elements in a simulation box of 120 Å in size, separated by a slit-like mesopore 51 Å in width in periodic boundary conditions. Colour scheme is the same as before.

volume of the system is consistent with the reference value. Here we focus on one particular realization of this model, shown in Figure 7 with the structural characteristics provided in Table 3 (in comparison with the reference data and the original microporous model).

The system considers an original packing of elements, duplicated in x-direction, giving the length of microporous region of 120 Å. The total length of the system in x-direction is 171 Å (placed in periodic boundary conditions), leading to slit-like spaces between microporous regions of about 51 Å wide. This pore size is clearly larger than what is detected in the real

Table 3. Structural characteristics of BAM-109 from experiments and from the model.

	N	S (m^2/g)	V (cm^3/g)	ρ (g/cm^3)	PLD (Å)	LP (Å)
Experiments	*	1383	Micro 0.5163 Total 1.045	*	*	*
Micro	395	990.62	0.509	0.808	4.36	8.45
Micro–Meso	395	1262.28	Micro 0.516 Total 1.042	0.567	45.42	49.64

*Property not applicable, or provided.

materials and further tuning of the model could be performed but this was not attempted here.

In this table N is the number of structural elements in the system, S is the surface area, V is the micropore volume (the experimental value has been obtained from QSDFT analysis of argon adsorption data at 87 K), ρ is the density of the material, PLD is the pore limiting diameter and LP is the diameter of the largest pore in the structure.

As can be seen from Table 3, the system has a very good agreement with the reference values in terms of the total and micropore volumes (the latter calculated as the difference between the total volume and the volume of the mesopore, $60\,\text{Å} \cdot 60\,\text{Å} \cdot 51\,\text{Å}$). The edges of the micropore region are now being exposed and this leads to an increase in the accessible surface area bringing it much closer to the reference value.

Figure 8 shows the results for argon adsorption at 87 K. The model substantially improves in the low and medium pressure regions and in capturing the isotherm plateau. However, the model fails to correctly capture the region of capillary condensation, exhibiting substantial hysteresis and the adsorption branch extending beyond the bulk condensation pressure (not shown). The desorption branch indicates that the total volume of the system is captured reasonably well (within 7%).

Interestingly, no substantial improvement is observed in application of the model to carbon dioxide adsorption (Figure 9). Given the results of the previous section we do not attempt to simulate adsorption of water in this model.

We conclude this section with the predictions for the volume of perfluorohexane adsorption at 273 K, provided in Figure 10 (numerical values of loading for the microporous and micro-mesoporous models are provided in Table 4 for comparison for the three reference values of the relative pressure).

As expected, the loading of perfluorohexane is diminished at very low pressures, compared to the purely microporous model. This is because the exposed surfaces provide less attractive regions for adsorption compared to micropores. On the other hand at higher pressures (0.3, 0.6) where the microporous region of the system is fully filled, additional adsorption occurs in the mesopore region, although it is underestimated compared to the real material due to unrealistically large size of the mesopore. Compared to the experimental results, the proposed model shows a generally correct trend in adsorption loading up to relative pressures of 0.7. The most important deficiency of the model is lack of pores in 10–20 Å (large micropore) region, making the model too microporous. As a result, the model underestimates the amount of perfluorohexane adsorbed at 273 K, throughout the whole pressure range and by about 20% on average for the three reference points. Furthermore, at relative pressures above 0.7, the model fails to capture a continuous, steep rise in adsorption

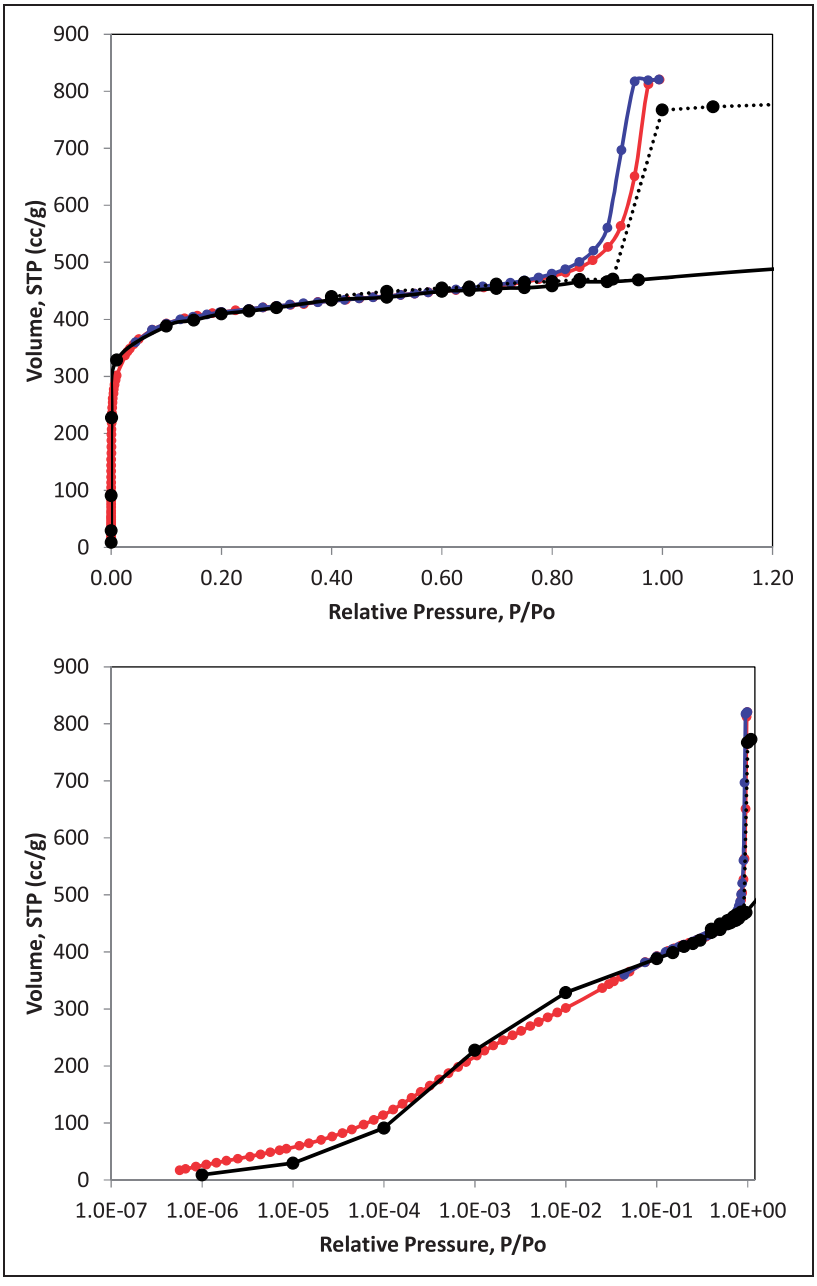

Figure 8. Sorption isotherms for argon at 87 K. Red and blue symbols and lines are the experimental adsorption and desorption isotherms, respectively. Black symbols and line are molecular simulation results. Dashed black line corresponds to the simulated desorption isotherm. The bottom figure plots the same comparison, using the logarithmic scale for relative pressure.

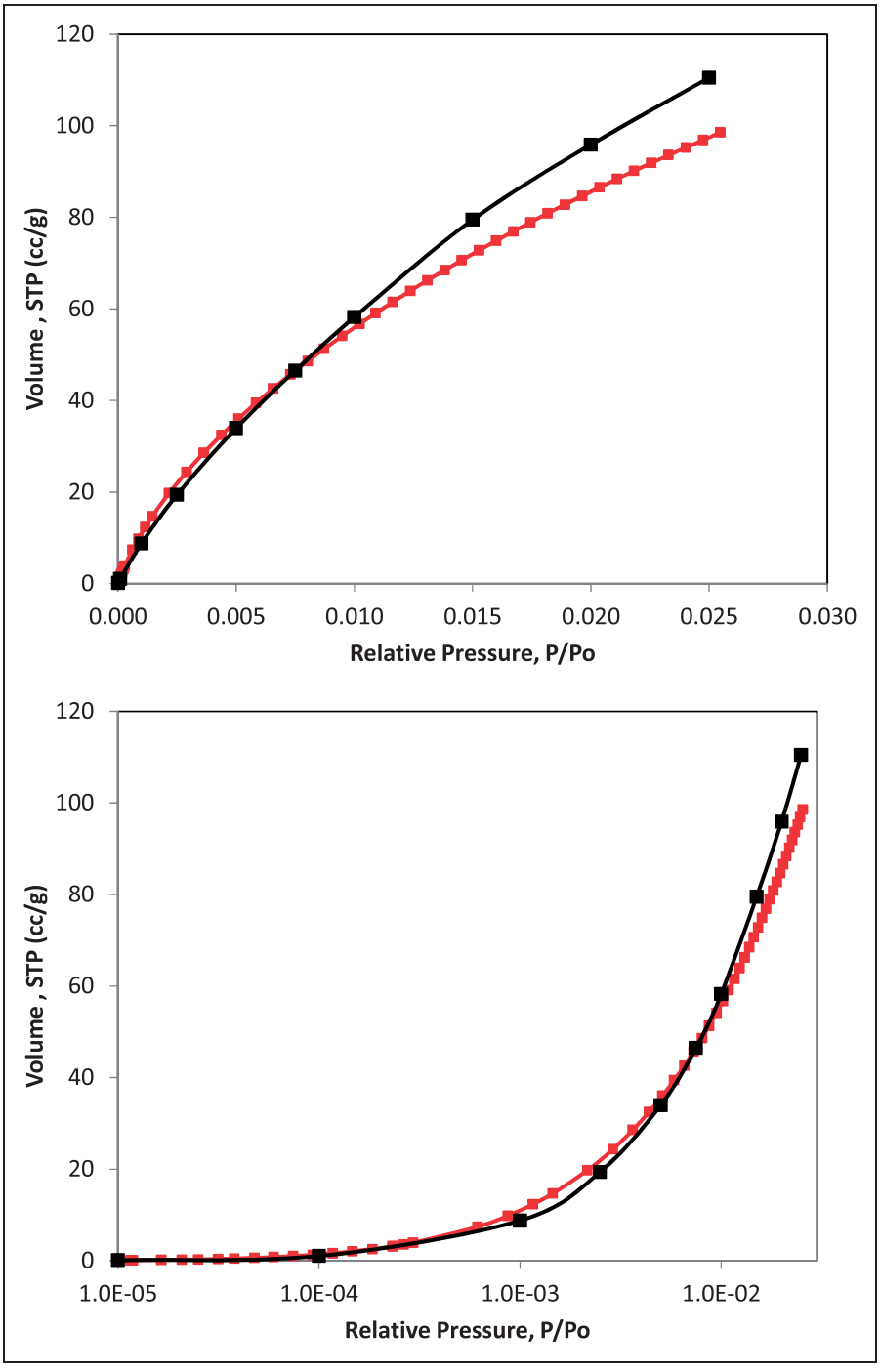

Figure 9. Adsorption isotherms for carbon dioxide at 273 K. Red symbols and line are the experimental results. Black symbols and line are molecular simulation results on the micro–mesoporous model of BAM-109. The bottom figure plots the same comparison, using the logarithmic scale for relative pressure.

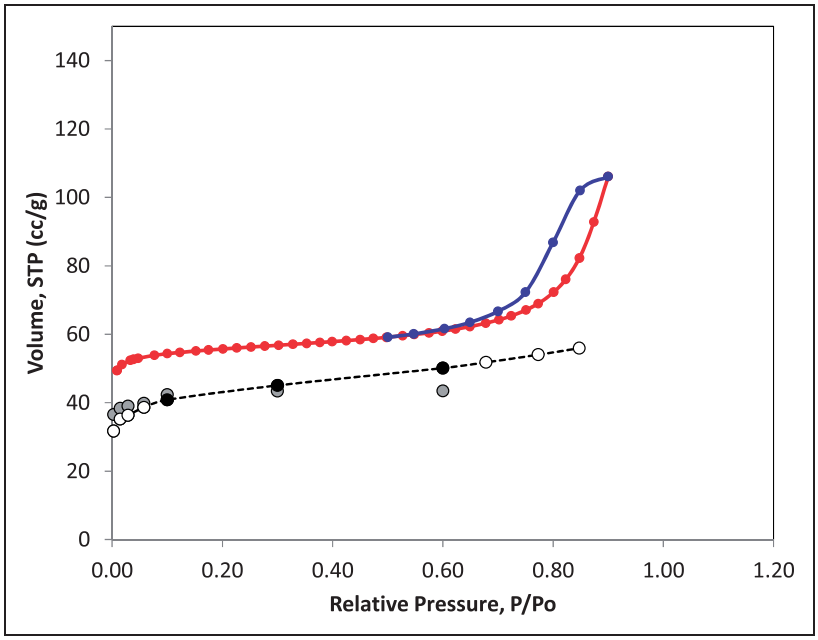

Figure 10. Adsorption isotherms of perfluorohexane in mesoporous model of BAM-109 at 273 K. Red and blue symbols are experimental reference results for adsorption and desorption, respectively. Lines of the matching colours are for eye guidance only. Black circles are simulation predictions at required values of relative pressure (0.1, 0.3 and 0.6). White circles are simulation predictions at other values of relative pressure. Simulation points are connected by dashed black line for eye guidance. Grey circles are predictions from the microporous model.

Table 4. Volume of perfluorohexane (cm^3/g STP) adsorbed in a model BAM-109 structure at 273 K as a function of relative pressure at target reference values. P_0(T = 273 K, TraPPE) = 34.8 kPa, see SI. Statistical error in loading at target pressures does not exceed 3%.

P/P_0	Micro V (cm^3/g STP)	Micro–Meso V (cm^3/g STP)
0.100	42.38	40.84
0.300	43.37	45.05
0.600	43.43	50.12

density associated with capillary condensation in mesopores (which also leads to the adsorption hysteresis on desorption in experiments). This is, of course, associated with the oversimplified model for the mesoporosity represented here effectively with a single very large pore of about 5 nm. Capillary condensation in this pore will be shifted towards higher pressures compared to that in the distribution of smaller pores in the actual material. Given the tendency of the Monte Carlo simulations to further overestimate the limits of metastability in simple slit pores on adsorption and desorption branches, we expect

that if continued this isotherm would have a steep jump in density at higher pressures (probably above the relative pressure of one), with the complete isotherm looking similar to that of argon at 87 K (Figure 8).

Conclusions

Given a very crude, first pass at the model development, the results presented in Figure 10 are surprisingly reasonable. As has been already discussed, the most important deficiency of the model is lack of pores in 10–20 Å (large micropore) region. This makes the model too microporous, with some of the regions of the porous space accessible to argon and carbon dioxide, but not to more bulky perfluorohexane. As a result, the amount of perfluorohexane adsorbed is underestimated at 273 K. Although further avenues for model improvement are available (more systematic tuning of solid–fluid interactions; construction of a model based on two types of structural elements of different size with a view to create more pores in 10–20 Å band), these have not been attempted here. An oversimplified representation of mesoporosity leads to the absence of continuous capillary condensation in the expected pressure range. A distribution of mesopores, more accurately reflecting the PSD would possibly alleviate these differences. In summary, the results of the Eighth Industrial Fluid Properties Simulation Challenge highlight that accurate prediction of adsorption in activated carbon still remains a substantial problem for molecular simulation.

Declaration of Conflicting Interests

The author(s) declared no potential conflicts of interest with respect to the research, authorship, and/or publication of this article.

Funding

The author(s) received no financial support for the research, authorship, and/or publication of this article.

References

Bandosz TJ, Biggs MJ, Gubbins KE, et al. (2003) Molecular models of porous carbons. In: Radovic LR (ed.) *Chemistry and Physics of Carbon*. Vol. 28. New York: Marcel Dekker.

Becke AD (1993) Density-functional thermochemistry III: The role of exact exchange. *Journal of Chemical Physics* 98: 5648.

Biggs MJ and Buts A (2006) Virtual porous carbons: What they are and what they can be used for. *Molecular Simulation* 32: 579.

Breneman CM and Wiberg KB (1990) Determining atom-centered monopoles from molecular electrostatic potentials. The need for high sampling density in formamide conformational analysis. *Journal of Computational Chemistry* 11: 361.

Brennan JK, Bandosz TJ, Thomson KT, et al. (2001) Water in porous carbons. *Colloids and Surfaces A: Physicochemical and Engineering Aspects* 187–188: 539.

Brennan JK, Thomson KT and Gubbins KE (2002) Adsorption of water in activated carbons: Effects of pore blocking and connectivity. *Langmuir* 18: 5438.

Brunauer S, Emmett PH and Teller E (1938) Adsorption of gases in multimolecular layers. *Journal of American Chemical Society* 60: 309.

Coasne B, Gubbins KE, Hung FR, et al. (2006) Adsorption and structure of argon in activated porous carbons. *Molecular Simulation* 32: 557.

Cracknell R, Nicholson D, Tennison S, et al. (1996) Adsorption and selectivity of carbon dioxide with methane and nitrogen in slit-shaped carbonaceous micropores: Simulation and experiment. *Adsorption* 2: 193.

Di Biase E and Sarkisov L (2015) Molecular simulation of multi-component adsorption processes related to carbon capture in a high surface area, disordered activated carbon. *Carbon* 94: 27.

Di Biase E and Sarkisov L (2013) Systematic development of predictive molecular models of high surface area activated carbons for adsorption applications. *Carbon* 64: 262.

Do DD and Do HD (2006) Modeling of adsorption on nongraphitized carbon surface: GCMC simulation studies and comparison with experimental data. *Journal of Physical Chemistry B* 110: 17531.

Dubinin MM and Radushkevich LV (1947) *Proceedings of the Academy of Sciences, Physical Chemistry Section, U.S.S.R.* 55: 331.

Ebner AD and Ritter JA (2009) State-of-the-art adsorption and membrane separation processes for carbon dioxide production from carbon dioxide emitting industries. *Separation Science and Technology* 44: 1273.

Everett DH and Powl JC (1976) Adsorption in slit-like and cylindrical micropores in the henry's law region. A model for the microporosity of carbons. *Journal of the Chemical Society, Faraday Transactions 1: Physical Chemistry in Condensed Phases* 72: 619.

Ewald PP (1921) Die Berechnung optischer und elektrostatischer Gitterpotentiale. *Annalen der Physik* 369: 253.

Fennel CJ and Gezelter D (2006) Is the Ewald summation still necessary? Peirwise alternatives to the accepted standard for long-range electrostatics. *Journal of Chemical Physics* 124: 234104.

Frenkel D and Smit B (2002) *Understanding Molecular Simulation: From Algorithms to Applications*. San Diego: Academic Press.

Frisch MJT, Schlegel HB, Scuseria GE, et al. (2009) Gaussian 03.

Gelb LD, Gubbins KE, Radhakrishnan R, et al. (1999) Phase separation in confined systems. *Reports on Progress in Physics* 62: 1573.

Gotzias A, Tylianakis E, Froudakis G, et al. (2012) Theoretical study of hydrogen adsorption in oxygen functionalized carbon slit pores. *Microporous Mesoporous Materials* 154: 38.

Gupta A, Chempath S, Sanborn MJ, et al. (2003) Object-oriented programming paradigms for molecular modeling. *Molecular Simulation* 29: 29.

Harris PJF (2004) Fullerene-related structure of commercial glassy carbons. *Philosophical Magazine* 84: 3159.

Harris PJF (2005) New Perspectives on the structure of graphitic carbons. *Critical Reviews in Solid State and Materials Sciences* 30: 235.

Harris PJF, Burian A and Duber S (2000) High-resolution electron microscopy of a microporous carbon. *Philosophical Magazine Letters* 80: 381.

Harris PJF and Tsang SC (1997) High-resolution electron microscopy studies of non-graphitizing carbons. *Philosophical Magazine A* 76: 667.

Harrison A, Cracknell RF, Krueger-Venus J, et al. (2014) Branched versus linear alkane adsorption in carbonaceous slit pores. *Adsorption—Journal of the International Adsorption Society* 20: 427.

Hawelek L, Brodka A, Dore JC, et al. (2008) Fullerene-like structure of activated carbons. *Diamond and Related Materials* 17: 1633.

Heuchel M, Davies GM, Buss E, et al. (1999) Adsorption of carbon dioxide and methane and their mixtures on an activated carbon: Simulation and experiment. *Langmuir* 15: 8695.

Hirschfelder JO, Curtiss CF and Bird RB (1954) *Molecular Theory of Gases and Liquids*. New York: Wiley & Sons.

Jagiello J and Olivier JP (2009) A simple two-dimensional NLDFT model of gas adsorption in finite carbon pores: Application to pore structure analysis. *Journal of Physical Chemistry C* 113: 19382.

Jagiello J and Schwarz JA (1993) Relationship between energetic and structural heterogeneity of microporous carbons determined on the basis of adsorption potentials in model micropores. *Langmuir* 9: 2513.

Jorge M and Seaton NA (2003) Predicting adsorption of water/organic mixtures using molecular simulation. *AIChE Journal* 49: 2059.

Jorge M, Seaton NA and Rodriguez-Reinoso F (2002) Characterisation of the surface chemistry of activated carbon by molecular simulation of water adsorption. In: Rodriguez-Reinoso F, McEnaney B, Rouquerol J and Unger K (eds) *Studies in Surface Science and Catalysis*, Amsterdam: Elsevier, pp.131–138.

Jorgensen WL and Madura JD (1985) Adsorption on edge-functionalized bilayer graphene nanoribbons: Assessing the role of functional groups in methane uptake. *Molecular Physics* 56: 1381.

Kandagal VS, Pathak A, Ayappa KG, et al. (2012) Adsorption on edge-functionalized bilayer graphene nanoribbons: Assessing the role of functional groups in methane uptake. *Journal of Physical Chemistry C* 116: 23394.

Kaneko K, Cracknell RF and Nicholson D (1994) Nitrogen adsorption in slit pores at ambient temperatures: Comparison of simulation and experiment. *Langmuir* 10: 4606.

Klauda JB, Jiang J and Sandler SI (2004) An ab Initio study on the effect of carbon surface curvature and ring structure on $N_2(O_2)$-carbon intermolecular potentials. *Journal of Physical Chemistry B* 108: 9842.

Kowalczyk P, Gauden PA, Terzyk AP, et al. (2012) Displacement of methane by coadsorbed carbon dioxide is facilitated in narrow carbon nanopores. *Journal of Physical Chemistry C* 116: 13640.

Kumar A, Lobo RF and Wagner NJ (2011) Grand canonical Monte Carlo simulation of adsorption of nitrogen and oxygen in realistic nanoporous carbon models. *AIChE Journal* 57: 1496.

Kumar KV, Müller EA and Rodríguez-Reinoso F (2012) Effect of pore morphology on the adsorption of methane/hydrogen mixtures on carbon micropores. *Journal of Physical Chemistry C* 116: 11820.

Lithoxoos GP, Peristeras LD, Boulougouris GC, et al. (2012) Monte Carlo simulation of carbon monoxide, carbon dioxide and methane adsorption on activated carbon. *Molecular Physics* 110: 1153.

Liu J-C and Monson PA (2005) Molecular modeling of adsorption in activated carbon: Comparison of Monte Carlo simulations with experiment. *Adsorption* 11: 5.

Liu JC and Monson PA (2006) Monte Carlo simulation study of water adsorption in activated carbon. *Industrial and Engineering Chemistry Research* 45: 5649.

Liu Y and Wilcox J (2012) Molecular simulation of CO_2 adsorption in micro- and mesoporous carbons with surface heterogeneity. *International Journal of Coal Geology* 104: 83.

Lucena SMP, Paiva CAS, Silvino PFG, et al. (2010) The effect of heterogeneity in the randomly etched graphite model for carbon pore size characterization. *Carbon* 48: 2554.

McCallum CL, Bandosz TJ, McGrother SC, et al. (1998) A molecular model for adsorption of water on activated carbon: Comparison of simulation and experiment. *Langmuir* 15: 533.

Macedonia MD and Maginn EJ (1999) A biased grand canonical Monte Carlo method for simulating adsorption using all-atom and branched united atom models. *Molecular Physics* 96: 1375.

Müller EA, Rull LF, Vega LF, et al. (1996) Adsorption of water on activated carbons: A MOLECULAR SIMULATION STudy. *Journal of Physical Chemistry* 100: 1189.

Neimark AV, Lin YZ, Ravikovitch PI, et al. (2009) Quenched solid density functional theory and pore size analysis of micro-mesoporous carbons. *Carbon* 47: 1617.

Nguyen TX, Cohaut N, Bae J-S, et al. (2008) New method for atomistic modeling of the microstructure of activated carbons using hybrid reverse Monte Carlo simulation. *Langmuir* 24: 7912.

Oberlin A, Villey M and Combaz A (1980) Influence of elemental composition on carbonization: Pyrolysis of kerosene shale and kuckersite. *Carbon* 18: 347.

Palmer JC, Brennan JK, Hurley MM, et al. (2009) Detailed structural models for activated carbons from molecular simulation. *Carbon* 47: 2904.

Pinto da Costa JMC, Cracknell RF, Seaton NA, et al. (2011) Towards predictive molecular simulations of normal and branched alkane adsorption in carbonaceous engine deposits. *Carbon* 49: 445.

Potoff JJ and Siepmann JI (2001) Vapor–liquid equilibria of mixtures containing alkanes, carbon dioxide, and nitrogen. *AIChE Journal* 47: 1676.

Radovic LR (2004) *Chemistry and Physics of Carbon*. Boca Raton: CRC Press.

Radovic LR and Bockrath B (2005) On the chemical nature of graphene edges: Origin of stability and potential for magnetism in carbon materials. *Journal of American Chemical Society* 127: 5917.

Ravikovitch PI, Vishnyakov A, Russo R, et al. (2000) Unified approach to pore size characterization of microporous carbonaceous materials from N-2, Ar, and CO_2 adsorption isotherms. *Langmuir* 16: 2311.

Samanta A, Zhao A, Shimizu GKH, et al. (2012) Post-combustion CO_2 capture using solid sorbents: A review. *Industrial and Engineering Chemistry Research* 51: 1438.

Samios S, Stubos AK, Kanellopoulos NK, et al. (1997) Determination of micropore size distribution from grand canonical monte carlo simulations and experimental CO_2 isotherm data. *Langmuir* 13: 2795.

Sarkisov L and Harrison A (2011) Computational structure characterisation tools in application to ordered and disordered porous materials. *Molecular Simulation* 37: 1248.

Segarra EI and Glandt ED (1994) Model microporous carbons - microstructure, surface polarity and gas-adsorption. *Chemical Engineering Science* 49: 2953.

Severson BL and Snurr RQ (2007) Monte Carlo simulation of n-alkane adsorption isotherms in carbon slit pores. *Journal of Chemical Physics* 126.

SI: http://homepages.ed.ac.uk/lsarkiso/Sarkisov_8th_fluid_property_challenge_AST_SI.htm.

Silvestre-Albero J, Silvestre-Albero A, Rodríguez-Reinoso F, et al. (2012) Physical characterization of activated carbons with narrow microporosity by nitrogen (77.4 K), carbon dioxide (273 K) and argon (87.3 K) adsorption in combination with immersion calorimetry. *Carbon* 50: 3128.

Snurr RQ, Bell AT and Theodorou DN (1993) Prediction of adsorption of aromatic hydrocarbons in silicalite from grand canonical Monte Carlo simulations with biased insertions. *Journal of Physical Chemistry* 97: 13742.

Steele WA (1978) The interaction of rare gas atoms with graphitized carbon black. *Journal of Physical Chemistry* 82: 817.

Sweatman MB and Quirke N (2001) Characterization of porous materials by gas adsorption at ambient temperatures and high pressure. *Journal of Physical Chemistry B* 105: 1403.

Sweatman MB and Quirke N (2005) Gas adsorption in active carbons and the slit-pore model 1: Pure gas adsorption. *Journal of Physical Chemistry B* 109: 10381.

Sweatman MB, Quirke N, Zhu W, et al. (2006) Analysis of gas adsorption in Kureha active carbon based on the slit pore model and Monte-Carlo simulations. *Molecular Simulation* 32: 513.

Tenney CM and Lastoskie CM (2006) Molecular simulation of carbon dioxide in chemically and structurally heterogeneous porous carbons. *Environmental Progress* 25: 343.

Terzyk AP, Furmaniak S, Harris PJF, et al. (2007) How realistic is the pore size distribution calculated from adsorption isotherms if activated carbon is composed of fullerene-like fragments? *Physical Chemistry Chemical Physics* 9: 5919.

Thomson KT and Gubbins KE (2000) Modeling structural morphology of microporous carbons by reverse Monte Carlo. *Langmuir* 16: 5761.

Vega LF (2007) Structural characterization of nano- and mesoporous materials by molecular simulations. In: Balbuena PB and Seminario JM (eds) *Nanomaterials: Design and Simulation*. Amsterdam: Elsevier.

Vishnyakov A, Piotrovskaya E and Brodskaya E (1998) Capillary Condensation and Melting/Freezing Transitions for Methane in Slit Coal Pores. *Adsorption* 4: 207.

Walters JK, Rigden JS and Newport RJ (1995) Capillary condensation and melting/freezing transitions for methane in slit coal pores. *Physica Scripta* T57: 137.

Wang QA, Luo JZ, Zhong ZY, et al. (2011) CO_2 capture by solid adsorbents and their applications: current status and new trends. *Energy and Environmental Science* 4: 42.

Wongkoblap A and Do DD (2006) The effects of energy sites on adsorption of Lennard-Jones fluids and phase transition in carbon slit pore of finite length a computer simulation study. *Journal of Colloid and Interface Science* 297: 1.

Wongkoblap A and Do DD (2007) Characterization of Cabot non-graphitized carbon blacks with a defective surface model: Adsorption of argon and nitrogen. *Carbon* 45: 1527.

Zhang L and Siepmann JI (2005) Pressure dependence of the vapor-liquid-liquid phase behavior in ternary mixtures consisting of n-alkanes, n-perfluoroalkanes, and carbon dioxide. *Journal of Physical Chemistry B* 109: 2911.